

# Radiography Open

ISSN: 2387-3345

Vol 7, No 1 (2021)

<https://doi.org/10.7577/radopen.4491>

## Analysis of the iodine distribution map in patients with diagnosis of pulmonary embolism: Initial results

Cecilia Muñoz Barabino<sup>1\*</sup>, Anghelo Silencio Higa<sup>1</sup>, Isna Larico Pampamallco<sup>1</sup>

<sup>1</sup> Departamento Académico de Tecnología Médica, Facultad de Medicina, Universidad Nacional Mayor de San Marcos. Lima, Perú.

\*Corresponding author e-mail address: [cmunozb@unmsm.edu.pe](mailto:cmunozb@unmsm.edu.pe)

**Keywords:** Iodine Mapping; Pulmonary Embolism; Dual Energy; Computed Tomography.

### Abstract

**Introduction:** The main evaluation of pulmonary embolism (PE) is clinical. Radiological studies are of great importance in diagnosis, Dual Energy Computed Tomography (DECT) is an alternative as a diagnostic method in pulmonary thromboembolism. The main objective was to determine the diagnostic advantage of using the Iodine Map in the detection of pulmonary thrombi.

**Methods:** Prospective study. Angiotomography images were acquired by dual energy and performed on a Discovery HD 750 Computed Tomography (GE) with GSI technology. Twenty-four images were processed on the AW VolumeShare 7 workstation (GE). The iodine map was represented with a colour scale. SPSS v.25 statistical software was used for interpretive analysis of the data.

**Results:** Two types of images were processed: simple monochromatic and monochromatic with iodine map. Thirty-four thrombi (21 occlusive and 13 partial) were found in the simple monochromatic images. Forty-one thrombi with perfusion defect were found in the monochromatic images processed with iodine map, pulmonary thrombi (70.73%), thrombi due to other pathology (17.07%) and thrombi produced by artifacts (12.20%). Both presented a statistically significant difference ( $p < .001$ ).

©2021 the author(s). This is an Open Access article distributed under the terms of the Creative Commons Attribution 4.0 International License (<http://creativecommons.org/licenses/by/4.0/>), allowing third parties to copy and redistribute the material in any medium or format and to remix, transform, and build upon the material for any purpose, even commercially, provided the original work is properly cited and states its license.

**Conclusion:** The radiologist physician had a better diagnostic accuracy, based on the partial or total detection of pulmonary thrombi through the distribution of the iodine map.

## Introduction

Pulmonary embolism or pulmonary thromboembolism (PE) is one of the most common pathologies in hospitals, also considered the third most frequent heart disease after acute myocardial infarction and cerebrovascular accident (CVA). (Alcocer G. et al. 2006) (Piazza & Goldhaber, 2010).

The incidence of PE worldwide is not clear; in the past decade it was 71-74.5 persons per 100,000 inhabitants in the United States, and it is estimated that the number of people suffering this disease is increasing every year. (Estrada & Garzona, 2015). In Spain is 154 cases per 100,000 inhabitants; the average age is 65 years, being more frequent in men and with an incidence that increases with age. (Simón-Montero et al., 2020)

Pulmonary thromboembolism is a life-threatening disease that occurs when blood clots (thrombi) that form elsewhere in the body migrate through the veins to the lung, where they become lodged in the pulmonary arteries. If the symptoms (shortness of breath, chest pain and cough) are not diagnosed in time, it can become a common cause of in-hospital death. (Torbick, A., & Perrier, A., 2008)

Imaging tests have become fundamental and are of great importance in the diagnosis of PE, from conventional chest radiography to more complex studies according to technological advances, such as angiotomography, considered the specific diagnostic test. (Noschang et al., 2018), (Oca, R., & Trinidad, C., 2013)

Dual-energy computed tomography (DECT), uses different energy spectral to differentiate materials and characterize tissues. It is based on the attenuation of different tissues at two different energy levels (80 kVp - 140 kVp) because tissues attenuate differently depending on the composition of their elements. (Forghani, R., et al., 2017)

There are several companies that manufacture DECT scanners, (Mc Collough, et al., 2015). General Electric Healthcare has GSI (Gemstone Spectral Imaging) technology with a single x-ray tube and one detector system, where the source performs a rapid change of energy (80-140 kVp) in the acquisition, based on the ultrafast kV switching and with a cycle time of 0.25 milliseconds. (Chandra & Langan, 2010)

The contribution is the generation of Material Decomposition Images (MDI), highlighting for PE diagnosis the Iodine Map or Iodine/Water (I/W) images, which analyse pulmonary perfusion in the lung parenchyma and thus provide not only a morphological view, also a functional view based on the distribution of Iodine. This is an important tool for the evaluation of any perfusion defect generated in a vessel by an occlusive partial or complete obstruction of the pulmonary artery somewhere in its extension. The benefits are obtained

without increasing the dose to the patient or the amount of contrast medium used. (Weidman et al., 2018)

(Bustos Fiore et al., 2018) they described the usefulness of dual-energy CT for obtaining pulmonary perfusion maps that provide morphological and functional information in patients with pulmonary embolisms, concluding that the new dual-energy CT scanners are useful for detecting perfusion defects secondary to complete or partial obstruction of the pulmonary arteries. (Lu et al., 2010) demonstrated its use for detecting pulmonary embolisms in the subsegmental branches.

The experimental study by (Tang et al., 2013) found that histopathological findings as a reference standard, together with dual-energy CT-based vascular iodine analysis improves the sensitivity for detecting peripheral pulmonary thrombus compared to CT pulmonary angiography, although at the same time, there is a decrease in specificity and positive predictive value.

Finally, (Monti et al., 2021), performed a meta-analysis on the performance of dual-energy CT in acute pulmonary embolism, recommends that dual-energy computed tomography did not provide a better diagnostic performance than single-energy computed tomography (SECT) for the diagnostic performance than DECT for the detection of acute lobar and segmental PE, regardless of the use of different post-processing techniques.

Therefore, DECT or SECT can be used for the detection of acute lobar and segmental pulmonary embolism in terms of each patient, the advantages are potential of DECT in terms of subsegmental detection in the diagnosis of acute pulmonary embolism, radiation and contrast agent. (Henzler et al., 2012)

The main objective of this study was to determine the diagnostic advantage of using the Iodine Map in the diagnosis of pulmonary embolism, as well as to identify the main characteristics of pulmonary thrombi on monochromatic images, to analyse the perfusion defects evidenced on the Iodine Map and to determine the density of normal lung parenchyma and with perfusion defects generated by occlusive and partially occlusive thrombi.

## Methods

The study was non-experimental, cross-sectional, quantitative with prospective data collection. The investigation involved twenty-four pulmonary computed angiotomography studies acquired with DECT. The acquisition of the DECT angiotomography images was performed by scanning the patient only once and then the collected data were processed on the workstation with connection to the AW VolumeShare 7 workstation (GE). Studies with previous pneumonectomy were not included.

All DECT studies were performed in a dual-energy computerized tomography with a single radiation tube with fast kV-switching (Discovery CT750 HD - General Electric Healthcare),

Analysis of the iodine distribution map in patients with diagnosis of pulmonary embolism

pitch 1.375, rotation time of 0.50 seconds, 64 slice per rotation, slice thickness of 0.625 mm and the raw data acquired was reconstructed using standard (STD – low frequency) kernels.

The contrast medium was Iopamidol 300 mg/ml and the bolus technique was used for injection with a volume of 50 ml per study (20 ml for test bolus acquisition and 30 ml for acquisition of the Gemstone Spectral Imaging (GSI) study with a flow rate of 5.0 ml/s. The GSI acquisition starts with a 7-second delay after detect 100 mean Hounsfield units (HU) threshold. The reconstructed images for analysis were monochromatic at 70 KeV the energy.

The reference site was placed at the bifurcation of the pulmonary arteries.

Two radiological physicians with more than 10 years of professional experience, analyzed the images of the monochromatic and iodine maps, both without knowing the result of the other. The images were studies performed with dual-energy CT to discard a pulmonary thromboembolism.

The diagnoses were made by analysing the iodine concentration in the arteries, describing the location (right main artery, left main artery, right upper pulmonary lobe, right middle lobe, right lower lobe, left upper lobe and left lower pulmonary lobe), the level (pulmonary trunk, main branch, lobar branch, segmental branch and subsegmental branch) and the type of pulmonary thrombi (occlusive and partial occlusive).

The types of thrombi for this investigation are two, occlusive (when the thrombi obstruct completely the lumen of the vessel) and partial occlusive (when the thrombi do not obstruct the lumen completely).

The visual presentation of thrombi according to their shape on the iodine map was classified as: wedge-shaped, circumscribed and banded perfusion defects.

Wedge-shaped findings were considered only for the diagnosis of pulmonary embolism, circumscribed findings are related to other diseases (lung masses, atelectasis, etc.) and banded findings are related to beam hardening artifacts.

The findings evidenced in the iodine mapping analysis were compared with monochromatic images for the identification of new pulmonary thrombi.

On the other hand, quantitative measurements of normal parenchyma and parenchyma with perfusion defects were performed, were measured on iodine maps with mg/ml units (iodine concentration) and with an average of 0.10 cm<sup>2</sup> of the region of interest (ROI) the parenchyma with perfusion defect due to a thrombi and normal parenchyma. Those values were classified according the type of thrombi.

Additionally, CTDIvol and DLP values were collected from the studies performed, with ASiR (GE Healthcare) radiation dose reduction technology activated at "GS50 50%".

A descriptive and inferential statistical analysis was performed.

Dose information (CTDIvol and DLP) from CT angiotomography acquired during DECT acquisition was collected and tabulated only as a reference for the dosimetry of these techniques.

This research complies with ethical aspects, maintains the anonymity and confidentiality of the data collected, being used for research purposes only. In addition, it preserves the commitment to the authenticity of the results.

## Results

Findings in monochromatic imaging: A total of 34 pulmonary thrombi were identified in 24 DECT studies using 70 keV monochromatic imaging alone. The pulmonary thrombi were classified according to level, location and type (table 1).

**Table 1**

Characteristics of pulmonary thrombi

| <b>Characteristics of pulmonary thrombi in the monochrome image</b> |          |          |
|---|----------|----------|
|   | <b>N</b> | <b>%</b> |
|   | 1        | 2.78%    |
|   | 2        | 5.56%    |
| <b>Level</b>  | 7        | 19.44%   |
|   | 14       | 44.44%   |
|   | 10       | 27.78%   |
|   | 2        | 5.56%    |
|   | 1        | 2.78%    |
|   | 6        | 16.67%   |
| <b>Location</b>   | 5        | 13.89%   |
|   | 8        | 22.22%   |
|   | 8        | 22.22%   |
|   | 6        | 16.67%   |
|   | 13       | 36.11%   |
| <b>Type</b>   | 23       | 63.89%   |
| <b>Total</b>  | 36       | 100%     |

Regarding to the level of location of these pulmonary thrombi, it was found that 1 (2.94%) was located at the level of the pulmonary trunk, 2 (5.88%) at the level of the main branch, 7 (20.59%) at the level of the lobar branch, 14 (41.18%) at the level of the segmental branch and 10 (29.41%) at the level of the sub-segmental branch. Regarding to the location of the pulmonary thrombi, 2 (5.88%) were located in the right main artery, 1 (2.94%) in the left main artery, 6 (17.65%) in the right upper lobe, 4 (11.76%) in the right middle lobe, 7 (20.59%) in the right lower lobe, 8 (23.53%) in the left upper lobe and 6 (17.65%) in the left lower lobe. In addition, regarding to the type of occlusion, 13 (38.24%) were partial occlusives and 21 (61.76%) total occlusives.

Iodine Map Findings: A total of 24 Iodine Maps were analysed and 41 perfusion defects were identified; of these, 29 (70.73%) were wedge-shaped and consistent with PE (Figure 1), 7 (17.07%) circumscribed shape and consistent with other pathologies and 5 (12.20%) banded shape and consistent with the physical beam hardening artefact (table 2) (Figure 2).

**Table 2**

Perfusion defects on the Iodine Map

| Perfusion Defects in Iodine Map | N  | %      |
|---------------------------------|----|--------|
| Wedge shape                     | 29 | 70.73% |
| Shape Circumscribed shape       | 7  | 17.07% |
| Band shape                      | 5  | 12.20% |
| Total                           | 41 | 100%   |

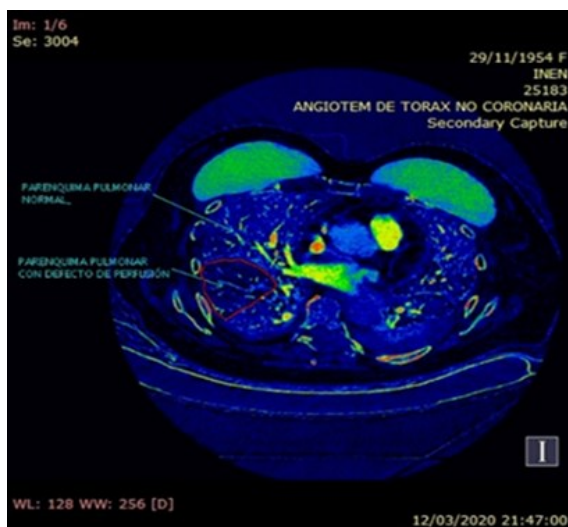


**Figure 1.**

Iodine map showing wedge-shaped perfusion defect consistent with pulmonary thromboembolism.

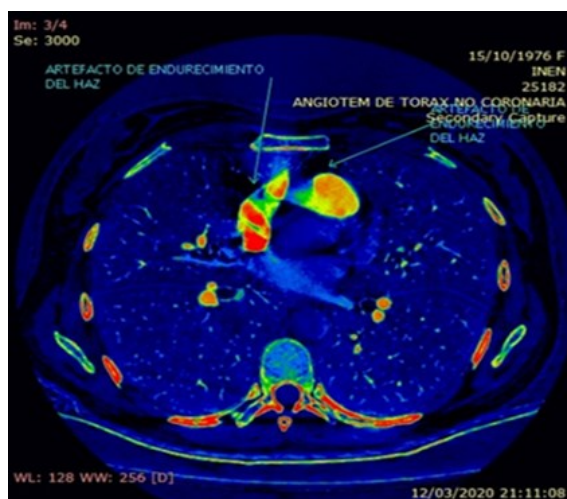


**Figure 2**

Iodine map showing band-shaped perfusion defect consistent with beam hardening artifact.

Comparison between monochromatic images and the Iodine Map finding: After a second reading of the monochromatic images and analysis of the Iodine Map, it was identified that, of the total number of pulmonary thrombi found at the beginning, 27 had perfusion defects; 20 were occlusive thrombi and 7 were partial occlusive thrombi, its mean without completely filling the diameter of the artery.

Additionally, 2 new pulmonary thrombi (5.56%) were identified with the help of the Iodine Map, were partial occlusive, I mean when the vessel lumen is not totally occluded and segmental level (table 3).

**Table 3.**

New pulmonary thrombi from the Iodine Map complementary to the monochrome images

| <b>New pulmonary thrombi from the iodine map complementary to the monochrome images</b> | <b>N</b>  | <b>%</b>      |
|---|-----------|---------------|
| Pulmonary thrombi identified without Iodine Map   | 34        | 94.4%         |
| New pulmonary thrombi identified with Iodine Map  | 2         | 5.6%          |
| <b>Total</b>  | <b>36</b> | <b>100.0%</b> |

The quantitative evaluation consisted in the measurement of the Iodine concentration in an elliptical ROI (Figure 3).

The Iodine Map density in the normal parenchyma had a minimum value of 0.88 mg/ml, maximum value of 2.79 mg/ml and average of  $1.65 \pm 0.66$  mg/ml. On the other hand, the density of the parenchyma with perfusion defects generated by pulmonary thrombi showed a minimum value of 0.12, maximum value of 1.02 and mean value of  $0.49 \pm 0.24$  mg/ml. Both groups showed significant statistical differences ( $p < .001$ ) (table 4).

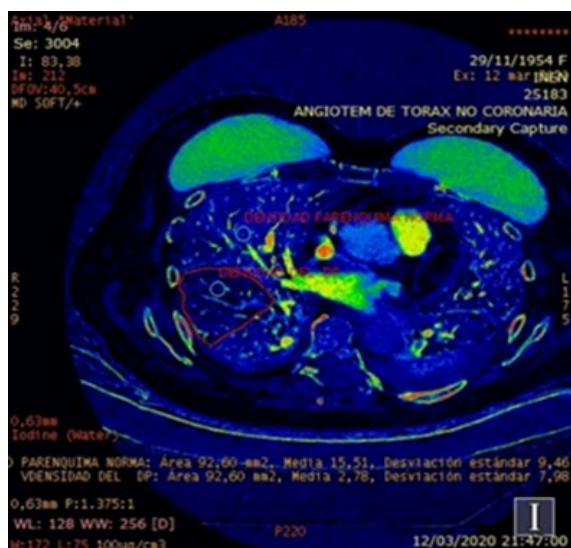


**Figure 3.**

Quantification of the density of the normal lung parenchyma and with perfusion defect in the Iodine Map.

**Table 4.**

Density of the lung parenchyma with perfusion defects consistent with PE and normal lung parenchyma

| Lung parenchyma                  | Density (mg/ml) |      |                    |      |      |       |
|----------------------------------|-----------------|------|--------------------|------|------|-------|
|                                  | Total           | Mean | Standard deviation | Mín  | Máx  | p<    |
| Normal parenchyma                | 29              | 1.65 | 0.66               | 0.88 | 2.79 |       |
| Parenchyma with Perfusion Defect | 29              | 0.49 | 0.24               | 0.12 | 1.02 | 0.001 |

\* Wilcoxon test

In addition, the density of the perfusion defects was differentiated according to the type of pulmonary thrombi. The density of the parenchyma with perfusion defect caused by total occlusive pulmonary thrombi had a minimum value of 0.12mg/ml, a maximum value of 0.66 mg/ml and a mean value of  $0.39 \pm 0.16$  mg/ml. Otherwise, in the parenchyma with perfusion defect caused by partial occlusive thrombi, had a minimum value of 0.56 mg/ml, a maximum value of 1.02 mg/ml and a mean value of  $0.80 \pm 0.18$ . Both groups also showed statistically significant variations ( $p < .001$ ) (table 5).

**Table 5.**

Density of perfusion defects generated by total occlusive and partial occlusive thrombi

| Pulmonary thrombus         | Density in lung parenchyma with perfusion defect |      |                    |      |      |       |
|----------------------------|--|------|--------------------|------|------|-------|
|                            | Total  | Mean | Standard deviation | Mín  | Máx  | p<    |
| Occlusive thrombus         | 22   | 0.39 | 0.16               | 0.12 | 0.66 | 0.001 |
| Partial occlusive thrombus | 7  | 0.8  | 0.18               | 0.56 | 1.02 |       |

\*Student's t for 2 independent samples

Dosimetry values: The CTDIvol and DLP mean value of DECT acquisitions were 6.22 mGy and 266.25 mGy.cm respectively, with minimum values of 5.08 mGy and 217.3 mGy.cm; and maximum values of 9.84 mGy and 381.99 mGy.cm. On the other hand, the values of the random conventional CT acquisition had as average 8.14 mGy and 315.42 mGy.cm of the CTDIvol and DLP respectively, minimum values of 7.01 mGy and 254.43 mGy.cm and maximum values of 11.04 mGy and 427.96 mGy.cm (table 6).

**Table 6.**

Dosimetric values of conventional and dual-energy computed tomography angiography studies.

| Modality                     | Dosimetric values |               |      |       |              |        |        |
|------------------------------|-------------------|---------------|------|-------|--------------|--------|--------|
|                              | Total             | CTDIvol (mGy) |      |       | DLP (mGy.cm) |        |        |
|                              |                   | mean          | Min  | Max   | mean         | Min    | Max    |
| Dual Energy Angiotomography  | 24                | 6.22          | 5.08 | 9.84  | 266.25       | 217.3  | 381.99 |
| Conventional Angiotomography | 24                | 8.14          | 7.01 | 11.04 | 315.42       | 254.43 | 427.96 |

## Discussion

The diagnosis of Pulmonary embolism must be timely and appropriate, the use of imaging tests is indispensable. Multidetector CT with contrast media is considered the Standard Gold test for the diagnosis of PE (Chien et al., 2019), but it only allows a morphological view of the pulmonary vessels and the identification of the pulmonary thrombi based on its visualisation. Analysis of lung perfusion and functional visualisation is also of great importance for a more accurate diagnosis of PE.

## Analysis of the iodine distribution map in patients with diagnosis of pulmonary embolism

The Iodine Map allows us to quickly show possible pulmonary thrombi by the variations in the parenchyma density that then can be contrasted on monochromatic images. Usually, perfusion defects related to pulmonary thrombi are wedge-shaped.

The pulmonary thrombi found according to the level of location were mainly in the segmental branch and in the sub segmental branch (Table 1), results that were similar to the previous study by (Weidman et al. 2018) On the other hand, according to the type of pulmonary thrombi found, we obtained a discrepancy between total occlusive thrombi over partial occlusive thrombi, caused by the difference in vessel caliber, in addition, Weidman et al. did not exclude any patients with DECT regardless of diagnosis, so it is possible that his group of patients had larger lesions overall. A large percentage of perfusion defects were caused by pulmonary thrombi followed by other pathologies.

Regarding the usefulness of the Iodine Map and the comparative analysis with the monochromatic image, two new pulmonary thrombi were identified (5.56%) that could not be visualised at the first review, these pulmonary thrombi were partial occlusive and located at segmental level. (Wu et al., 2012) also evaluated the iodine mapping study by finding 6% more pulmonary thrombi recommending that iodine density quantification can be used as a predictive factor to distinguish the presence or absence and severity of PE.

The quantitative analysis provided by the Iodine Map is also of great importance because it allows us to show the complementary information that a complete medical report requires. The study shown that the density of normal parenchyma had an average of  $1.65 \pm 0.66$  mg/ml, a value that was higher than the density of the parenchyma with perfusion defect caused by lung thrombi that had an average of  $0.49 \pm 0.24$  mg/ml, these results showed statistically significant differences ( $p < .001$ ). (Table 4)

Wu et al (2012), evaluated parenchymal density and defects caused by occlusive pulmonary thrombi, concluding that the density of perfusion defects analyzed quantitatively may be useful for the evaluation of post-treatment anticoagulation controls based on density variation.

Dose information (CTDIvol and DLP) from DECT acquisition was compiled and compared with the results of routine angiotomography to show the dosimetry of these techniques. The dual energy technique was shown to have a very significant decrease, a result similar to the study by (Henzer et al., 2012) in which a decrease in dose values was also found when using DECT. (Table 6). However, the increased information content and post-processing flexibility of DECT data open up additional avenues for substantial radiation dose savings in routine protocols. (Mi-Jin Kang et al., 2010). Table 3, demonstrates that the iodine distribution map offers a superior diagnostic advantage by diagnosing 5.6% in the detection of pulmonary embolism by DECT.

## Conclusion

An accurate diagnosis could save many lives, it is important to decide the diagnostic method chosen without harming the patient by overdiagnosis, so we need more information for good decision making, dual energy angiotomography is a radiological technique to detect small emboli that need treatment (Wiener et al., 2013).

The sample size was a limitation for the authors, for this reason, we present the initial experience based on a reduced population for perfusion in the Iodine Map.

Correlation studies comparing perfusion defects by dual-energy tomography with ventilation-perfusion (V/Q) scanning are recommended.

### Conflict of interest statement

None. This research did not receive any specific grant from funding agencies in the public, commercial, or not-for-profit sectors.

## References

Alcocer Gamba, MA., González Juárez, F., León González, S., Castro Montes, E., & Alejandro Romero, M. (2006). Tromboembolia pulmonar, un enfoque multidisciplinario. 65(2), 88–100.

Bustos Fiore, A., González Vázquez, M., Trinidad López, C., Mera Fernández, D., & Costas Álvarez, M. (2018). Perfusion defects in pulmonary perfusion iodine maps: Causes and semiology. *Radiología (English Edition)*, 60(4), 301–309.

<https://doi.org/10.1016/j.rxeng.2018.04.002>

Chandra, N., Langan, DA. (2010). Gemstone Detector: Dual Energy Imaging via Fast kVp Switching. *Dual Energy CT in Clinical Practice*. Berlin, Heidelberg: Springer Berlin Heidelberg; p 35–41. [DOI:10.1007/174\\_2010\\_35](https://doi.org/10.1007/174_2010_35)

Chien, C.-H., Shih, F.-C., Chen, C.-Y., Chen, C.-H., Wu, W.-L., & Mak, C.-W. (2019). Unenhanced multidetector computed tomography findings in acute central pulmonary embolism. *BMC Medical Imaging* 2019 19:1, 19(1), 1–8. <https://doi.org/10.1186/S12880-019-0364-Y>

Estrada Garzona, C. F., & Garzona Navas, A. F. Tromboembolismo pulmonar: Fisiopatología y diagnóstico. *Revista Clínica de la Escuela de Medicina UCR –HSJD* 2015; 5(2): 53–64.

Forghani, R., De Man, B., & Gupta, R. (2017). Dual-Energy Computed Tomography: Physical Principles, Approaches to Scanning. Usage, and Implementation: Part 1. *Neuroimaging clinics of North America*, 27(3), 371–384. <https://doi.org/10.1016/j.nic.2017.03.002>

Henzler T, Fink C, Schoenberg S, Schoepf J. Dual-Energy CT: Radiation Dose. Aspects. Alemania, AJR (2012), 199(5), S16-S25. DOI:[10.2214/AJR.12.9210](https://doi.org/10.2214/AJR.12.9210)

Lu, G. M., Wu, S. Y., Yeh, B. M., & Zhang, L. J. (2010). Dual-energy computed tomography in pulmonary embolism. The British journal of radiology, 83(992), 707–718. <https://doi.org/10.1259/bjr/16337436>. <https://doi.org/10.1259/bjr/16337436>

Mc Collough, C. H., Leng, S., Yu, L., & Fletcher, J. G. (2015). Dual- and Multi-Energy CT: Principles, Technical Approaches, and Clinical Applications. Radiology, 276(3), 637–653. <https://doi.org/10.1148/radiol.2015142631>

Mi-Jin Kang, Chang Min Park, Chang-Hyun Lee, Jin Mo Goo, Hyun Ju Lee. (2010). Dual-Energy CT: Clinical Applications in Various Pulmonary Diseases. RadioGraphics, 30:3, 685-698. <https://doi.org/10.1148/rg.303095101>

Monti, C. B., Zanardo, M., Cozzi, A., Schiaffino, S., Spagnolo, P., Secchi, F., De Cecco, C. N., & Sardanelli, F. (2021). Dual-energy CT performance in acute pulmonary embolism: a meta-analysis. European Radiology, 31(8), 6248–6258. <https://doi.org/10.1007/s00330-020-07633-8>

Noschang, Julia, Guimarães, Marcos Duarte, Teixeira, Diogo Fábio Dias, Braga, Juliana Cristina Duarte, Hochegger, Bruno, Santana, Pablo Rydz Pinheiro, & Marchiori, Edson. (2018). Pulmonary thromboembolism: new diagnostic imaging techniques. Radiología Brasileira, 51(3), 178-186. Epub May 28, 2018. <https://doi.org/10.1590/0100-3984.2017.0191>

Oca Pernas, R., & Trinidad, C. ECR (2013). Pulmonary Perfusion Iodine Map with Dual Energy CT: ¿Can It Predict Gravity and Extension of Acute Pulmonary Embolism? Initial Experience. European Society Radiology, C-1941. DOI:10.1594/ecr2013/C-1941

Piazza, G., & Goldhaber, S. Z. (2010). Management of submassive pulmonary embolism. Circulation, 122(11), 1124–1129. <https://doi.org/10.1161/CIRCULATIONAHA.110.961136>

Simón-Montero, E., Campos-Rivas, B., Guerra-García, M. M., Vírseda-Sacristán, A., Dorrego-López, M. A., & Charle-Crespo, Á. (2020). Evolución de la incidencia de la enfermedad tromboembólica venosa en Galicia durante diez años (2006-2015). Semergen, 46(5), 339–346. <https://doi.org/10.1016/j.semerg.2020.04.007>

Tang, C. X., Zhang, L. J., Han, Z. H., Zhou, C. S., Krazinski, A. W., Silverman, J. R., Schoepf, U. J., & Lu, G. M. (2013). Dual-energy CT based vascular iodine analysis improves sensitivity for peripheral pulmonary artery thrombus detection: An experimental study in canines.

European Journal of Radiology, 82(12), 2270–2278.

<https://doi.org/10.1016/j.ejrad.2013.06.021>

Torbick, A., & Perrier, A. (2008). Guías de práctica clínica de la Sociedad Europea de Cardiología. Guías de práctica clínica sobre diagnóstico y manejo del tromboembolismo pulmonar agudo. Revista Española De Cardiología, 61(12), 1330–52. Recuperado de <http://secardiologia.es/images/stories/documentos/guia-tep.pdf>

Weidman EK, Plodkowski AJ, Halpenny DF, Hayes SA, Perez-Johnston R, Zheng. (2018). Dual-Energy CT Angiography for Detection of Pulmonary Emboli: Incremental Benefit of Iodine Maps. Radiology, 289(2), 546-53. DOI:[10.1148/radiol.2018180594](https://doi.org/10.1148/radiol.2018180594)

Wiener, R. S., Schwartz, L. M., & Woloshin, S. (2013). When a test is too good: how CT pulmonary angiograms find pulmonary emboli that do not need to be found. BMJ, 347(7915). <https://doi.org/10.1136/BMJ.F3368>

Wu, H. W., Cheng, J. J., Li, J. Y., Yin, Y., Hua, J., & Xu, J. R. (2012). Pulmonary embolism detection and characterization through quantitative iodine-based material decomposition images with spectral computed tomography imaging. Investigative Radiology, 47(1), 85–91. <https://doi.org/10.1097/RLI.0B013E31823441A1>